Published in final edited form as:
Biochemistry. 2009 July 28; 48(29): 6898–6908. doi:10.1021/bi900605n.

Structure-based Design, Synthesis, Biochemical and Pharmacological Characterization of Novel Salvinorin A Analogues as Active State Probes of the κ-Opioid Receptor

Feng Yan[‡,†], **Ruslan V. Bikbulatov**[§], **Viorel Mocanu**[‖], **Nedyalka Dicheva**[‖], **Carol E. Parker**[‖], **William C. Wetsel**[⊥], **Philip D. Mosier**[◊], **Richard B. Westkaemper**[◊], **John A. Allen**[‡], **Jordan K. Zjawiony**[§,□], and **Bryan L. Roth**[‡,*]

[‡]Department of Pharmacology, University of North Carolina, Chapel Hill, NC 27599

[‖]UNC-Duke Proteomics Center, University of North, Carolina, Chapel Hill, NC 27599

[§]Department of Pharmacognosy, School of Pharmacy, University of Mississippi, University, MS 38677

[⊥]Department of Cell Biology, Duke University, Medical Center, Durham, NC 27710

[◊]Department of Medicinal Chemistry, Virginia Commonwealth University, Richmond, VA 23298

[□]National Center for Natural Products Research, Research Institute of Pharmaceutical Sciences, School of Pharmacy, University of Mississippi, University, MS 38677.

Abstract

Salvinorin A, the most potent naturally occurring hallucinogen, has gained increasing attention since the κ-opioid receptor (KOR) was identified as its principal molecular target by us (Roth et al, PNAS, 2002). Here we report the design, synthesis and biochemical characterization of novel, irreversible, salvinorin A-derived ligands suitable as active state probes of the KOR. Based on prior substituted cysteine accessibility and molecular modeling studies, $C315^{7.38}$ was chosen as a potential anchoring point for covalent labeling of salvinorin A-derived ligands. Automated docking of a series of potential covalently-bound ligands suggested that either a haloacetate moiety or other similar electrophilic groups could irreversibly bind with $C315^{7.38}$. 22-thiocyanatosalvinorin A (RB-64) and 22-chlorosalvinorin A (RB-48) were both found to be extraordinarily potent and selective KOR agonists *in vitro* and *in vivo*. As predicted based on molecular modeling studies, RB-64 induced wash-resistant inhibition of binding with a strict requirement for a free cysteine in or near the binding pocket. Mass spectrometry (MS) studies utilizing synthetic KOR peptides and RB-64 supported the hypothesis that the anchoring residue was $C315^{7.38}$ and suggested one biochemical mechanism for covalent binding. These studies provide direct evidence for the presence of a free cysteine in the agonist-bound state of KOR and provide novel insights into the mechanism by which salvinorin A binds to and activates KOR.

Salvinorin A, the active ingredient of the hallucinogenic plant *Salvia divinorum*, is the most potent known naturally-occurring hallucinogen (1,2). In 2002, we discovered that the κ-opioid receptor (KOR) was the molecular target for the actions of salvinorin A *in vitro* (3). Studies with KOR knock-out mice (4) unequivocally demonstrated that the KOR was also the site of

[†]This research was supported in part by NIH R01DA017204 (to B.L.R.) and the NIMH Psychoactive Drug Screening Program. J.A.A. was supported by Neurodevelopmental Training Program Fellowship Grant from the NIH.

Address correspondence to: Bryan L. Roth, M.D., Ph.D., Dept. of Pharmacology, 4072 Genetics Medicine Building, Medical School, University of North Carolina, Chapel Hill, NC 27599, Office: 919-966-7535, Fax: 919-843-5788, bryan_roth@med.unc.edu.

action of salvinorin A *in vivo*—a finding which has been widely replicated (see (5) and (6) for reviews). Subsequently, salvinorin A emerged as an attractive lead compound for drug discovery and during the past few years, hundreds of salvinorin A derivates have been synthesized (6). Some of these analogues present interesting pharmacological profiles, from full KOR agonist to partial δ-opioid receptor (DOR) or μ-opioid receptor (MOR) agonists and antagonists (7) (8) (9) (10) (11). However, most of the hundreds of analogues displayed decreased affinity (or even no affinity) to KOR. The present challenge now is to use the knowledge about salvinorin A–KOR interactions (12) (13) to design unique salvinorin A derivatives with novel pharmacological profiles and therapeutic potential. In recent years, covalently-bound ligands emerged as a new class of receptor ligands with unique pharmacological properties. The successful design of the covalently-bound ligands includes an allosteric modulator for $GABA_A$ receptor (14), fluorescently-tagged inhibitors for calcium-bound protein arginine deiminase 4 (PAD4) (15), selective kinase inhibitors (16,17), estradiols for estrogen receptor (18,19), and antagonists for *N*-methyl-D-aspartate (NMDA) receptor (a ligandgated cation channel) (20). This covalent-labeling method takes advantage of the chemically-reactive amino acids inside or close to the ligand binding site, and frequently the reactive group is a nucleophile. Because the recognition between the ligand and receptor is specific, proximity-accelerated covalent-labeling is expected to be highly selective. Introduction of a proper electrophilic group into the ligand structure is the key condition to promote covalent-labeling between the ligand and receptor. However, the structural variety of receptors and ligands creates uncertainty in choosing the optimal reactive group. Among the common reactive groups, halomethylketones, haloacetamides, isothiocyanates, Michael acceptors, aldol esters, nitrogen mustards and other electrophilic moieties have been used for covalently-bound ligands due to their relatively high reactivity under physiological conditions (*e.g.*, pH 7.4).

Our prior molecular modeling studies predicted that a chemically reactive cysteine ($C315^{7.38}$) would reside in or near salvinorin A's binding site in the agonist-bound state of the KOR (12,21) (13). Indeed, our prior studies showed there was a direct interaction between the acetoxy group of salvinorin A and $Y313^{7.36}$, a critical residue inside the binding pocket (12). Nearby, a water-accessible $C315^{7.38}$ is highly reactive to methanethiosulfonate (MTS) reagent (Figure 1A), as reported in the substituted cysteine accessibility method (SCAM) studies by Xu *et al*. (22) (23) and us (21). Because the $C315^{7.38}S$ mutation did not significantly affect salvinorin A's binding affinity, we predicted that $C315^{7.38}$ exists as a free cysteine rather than as a contributor to disulfide-bonds or the global structure of KOR. Theoretically, $C315^{7.38}$ could provide an anchoring point for covalent-labeling.

In this paper we describe molecular modeling studies which predict that 22-substituted salvinorin A derivatives will interact with $C315^{7.38}$. Based on these predictions 22-thiocyanatosalvinorin A (RB-64) and 22-chlorosalvinorin A (RB-48) were synthesized and found to be extraordinarily potent, selective and apparently irreversible KOR agonists *in vitro*. *In vivo* studies revealed RB-64 to be 20-fold more efficacious than salvinorin A. Mutagenesis experiments and biochemical studies with purified KOR peptides *in vitro* confirmed the mechanism of irreversible binding to be nucleophilic substitution to $C315^{7.38}$. These studies provide convincing evidence for a free cysteine in or near the agonist-bound active state of KOR.

EXPERIMENTAL PROCEDURES

Materials

Standard reagents were purchased from Sigma-Aldrich (St. Louis, MO). Some of the salvinorin A used as a standard in these studies was kindly provided by Dr. Thomas Prisinzano (University of Kansas).

Syntheses and Characterization of 22-Chlorosalvinorin A (RB-48) and 22-Thiocyanatosalvinorin A (RB-64)

Salvinorin B (25 mg, 64 μmol) and catalytic dimethylaminopyridine (DMAP) were dissolved in 5 mL of dichloromethane (DCM). Chloroacetyl chloride (10 mg, 90 μmol) was added, and the reaction mixture was stirred at room temperature for 2 hours. Then the solvents were evaporated *in vacuo*, and the residue was chromatographed on silica gel (hexane/ethyl acetate 3:1) to yield 22-chlorosalvinorin A (22.7 mg, 76% yield). White solid, mp 216–218 °C, α_D^{20} − 27.5 (*c* 0.08, MeCN), HRESIMS *m/z* $[M+H]^+$ 467.1457 (calcd for $C_{23}H_{27}ClO_8$ 466.1394). ^{13}C NMR (100 MHz, $CDCl_3$): δ 15.2, 16.4, 18.1, 30.5, 35.4, 38.1, 40.6, 42.1, 43.0, 51.2, 52.0, 53.3, 63.7, 71.9, 76.5, 108.5, 125.2, 139.6, 143.7, 166.6, 171.1, 171,4, 201.2; ^1H NMR (400 MHz, $CDCl_3$): δ 1.08 (s, 3H), 1.39 (s, 3H), 1.52–1.65 (m, 3H), 1.75 (m, 1H), 2.04–2.15 (m, 2H), 2.25–2.34 (m, 3H), 2.39 (dd, *J* = 5, 13 Hz, 1H), 2.76 (m, 1H), 3.70 (s, 3H), 4.18 (ABq, *J* = 15Hz, 2H), 5.20 (m, 1H), 5.43 (dd, *J* = 5, 12Hz, 1H), 6.36 (s, 1H), 7.37 (br s, 1H), 7.39 (s, 1H). 22-Chlorosalvinorin A (20 mg, 43 μmol) was dissolved in anhydrous ethanol (2 mL) with potassium thiocyanate (5.4 mg, 56 μmol). The reaction mixture was refluxed for 5 hours, allowed to reach room temperature, concentrated *in vacuo*. Water (2 mL) was then added and the reaction mixture was extracted with chloroform (three 5 mL portions). Solvents were removed *in vacuo*, and the mixture was separated by HPLC (C_{18} column, MeCN : H_2O (1:1), detection at 210 nm) to yield 22-thiocyanatosalvinorin A (16.6 mg, 79% yield). Semisolid, α_D^{20} − 32.5 (*c* 0.08, MeCN), HRESIMS *m/z* $[M+H]^+$ 490.1519 (calcd for $C_{24}H_{27}NO_8S$ 489.1452). IR (neat) 2160 cm^{-1} (SCN). ^{13}C NMR (100 MHz, $CDCl_3$): δ 15.2, 16.4, 18.1, 30.5, 34.5, 35.5, 38.1, 42.1, 43.3, 51.3, 52.0, 53.3, 64.0, 71.9, 76.9, 108.4, 110.3, 125.2, 139.5, 143.8, 165.4, 170.9, 171,2, 200.6; ^1H NMR (400 MHz, $CDCl_3$): δ 1.13 (s, 3H), 1.45 (s, 3H), 1.58–1.68 (m, 3H), 1.82 (m, 1H), 2.08–2.24 (m, 3H), 2.33–2.41 (m, 2H), 2.48 (dd, *J* = 5, 13 Hz, 1H), 2.79 (m, 1H), 3.75 (s, 3H), 3.89 (s, 2H), 5.22 (m, 1H), 5.53 (dd, *J* = 5, 12Hz, 1H), 6.40 (d, *J* = 1Hz, 1H), 7.41 (m, 1H), 7.44 (s, 1H). The synthesis scheme is shown in supplementary material Figure 1.

The other C22-substituted salvinorin A derivatives (RB-50, RB-55 RB-55-1, RB-55-2, RB-65, RB-66) presented in Table 1 were obtained in analogous way as RB-48 with the use of corresponding acyl chlorides.

22-Bromosalvinorin A (RB-50) was obtained in 55% yield using bromoacetyl chloride. Brownish solid, m.p. 214–215 °C (decomp.). RB-50 is a highly unstable at room temperature. It shows the spectral features analogous to those of 22-chlorosalvinorin A (RB-48), but its instability makes the accurate spectral measurements practically impossible. To minimize decomposition the products has to be stored in deep-freezer prior to binding assays.

(22-R,S)-22-Chloro-22-methylsalvinorin A (RB-55) was obtained in 83% yield using 2-chloropropionyl chloride. White solid, m.p. 198–200 °C, HRTOFIMS *m/z* $[M-H^+]$ 479.1464 (calcd for $C_{24}H_{28}ClO_8$ 479.1467). ^{13}C NMR (100 MHz, $CDCl_3$): δ 15.2, 16.4, 18.1, 21.6, 30.6, 35.4, 38.1, 42.1, 43.3, 51.3, 52.0, 52.3, 53.4, 64.0, 72.0, 76.0, 108.4, 125.2, 139.5, 143.7, 169.1, 171.0, 171.4, 200.8; ^1H NMR (400 MHz, $CDCl_3$): δ 1.14 (s, 3H), 1.45 (s, 3H), 1.52–1.71 (m, 4H), 1.77 (d, *J* = 4.0 Hz, 3H), 1.78–1.83 (m, 2H), 2.08 (dd, *J* = 11.5, 2.8 Hz, 1H), 2.13–2.22 (m, 2H), 2.37 (dd, *J* = 13.6, 7.1 Hz, 2H), 2.51 (dd, *J* = 13.4, 5.1 Hz, 1H), 2.78 (m, 1H), 3.74 (s, 3H), 4.51 (ABq, *J* = 7.0 Hz, 1H), 5.17 (m, 1H), 5.52 (dd, *J* = 11.6, 5.1 Hz, 1H), 6.39 (s, 1H), 7.40 (br s, 1H), 7.42 (s, 1H).

RB-55 was chromatographically separated to individual 22-*S* (RB-55-1) and 22-*R* (RB-55-2) epimers. Both epimers had the same spectral characteristic features. The structure of 22-*S* (RB-55-1) isomer was independently confirmed by X-ray crystallography.

22-Methoxysalvinorin A (RB-65) was obtained in 79% yield using methoxyacetyl chloride. Amorphous solid. HRTOFMS *m/z* [M-H$^+$] 461.1813 (calcd for $C_{24}H_{29}O_9$ 461.1806). ^{13}C NMR (100 MHz, $CDCl_3$): δ 15.1, 16.3, 18.1, 30.6, 35.3, 37.9, 42.0, 42.9, 51.0, 51.9, 53.2, 59.3, 63.5, 69.3, 71.9, 75.2, 108.5, 125.2, 139.5, 143.6, 169.4, 171.2, 171,5, 201.6; ^{1}H NMR (400 MHz, $CDCl_3$): δ 1.03 (s, 3H), 1.36 (s, 3H), 1.48–1.61 (m, 3H), 1.69 (dd, *J* = 10.8, 8.0 Hz, 1H), 1.99–2.11 (m, 2H), 2.19–2.28 (m, 3H), 2.38 (dd, *J* = 13.5, 5.1 Hz, 1H), 2.73 (dd, *J* = 15.4, 7.4 Hz, 1H), 3.40 (s, 3H), 3.65 (s, 3H), 4.09 (ABq, *J* = 16.6 Hz, 2H), 5.19 (t, *J* = 10.0 Hz, 1H), 5.43 (dd, *J* = 11.7, 5.0 Hz, 1H), 6.32 (s, 1H), 7.33 (br s, 1H), 7.36 (s, 1H).

22-Dichlorosalvinorin A (RB-66) was obtained in 86% yield using dichloroacetyl chloride. Amorphous solid, ^{13}C NMR (100 MHz, CDCl^3): δ 15.1, 16.4, 18.1, 30.3, 35.4, 38.1, 42.1, 42.9, 51.2, 52.0, 53.2, 63.8, 71.9, 76.7, 108.5, 109.3, 125.1, 139.6, 143.7, 163.8, 171.0, 171.2, 200.2; ^{1}H NMR (400 MHz, $CDCl_3$): δ 1.11 (s, 3H), 1.41 (s, 3H), 1.52–1.65 (m, 3H), 1.78 (dd, *J* = 10.2, 2.5 Hz, 1H), 2.04–2.15 (m, 2H), 2.27 (s, 1H), 2.33–2.45 (m, 3H), 2.78 (m, 1H), 3.72 (s, 3H), 5.20 (t, *J* = 10.0 Hz, 1H), 5.45 (dd, *J* = 11.7, 5.0 Hz, 1H), 6.07 (s, 1H), 6.38 (s, 1H), 7.39 (br s, 1H), 7.41 (s, 1H).

[^{35}S]GTPγS Binding Assay

Ten different concentrations of testing compounds in appropriate concentrations were made in the binding buffer (50 mM Tris·HCl, 100 mM NaCl, 10 mM $MgCl_2$, 1 mM EDTA, pH 7.4). The [^{35}S]GTPγS assay was set up in 96-well sample plates (Wallac) designed for the 1450 MicroBeta Counter (PerkinElmer). 50 μL drug solution, 50 μl [^{35}S]GTPγS (PerkinElmer, 1250 Ci/mmol), 50 μL membrane plus 20 μM guanosine 5'-diphosphate (GDP) were added to 96-well plates and incubated for 20 min at room temperature, then 50 μL beads (FlashBlue, PerkinElmer, stock = 100 mg/ml, 110 μL stock solution/plate) were added to the mixture. The plates were shaken for half an hour on a titer plate shaker (Lab-line Instruments, Inc.), spun down at 1000 rpm (~270 *g*) for 2 min, and counted using an ^{35}S protocol with a 1450 MircoBeta Counter (PerkinElmer).

Transient and Stable Expression of KOR

HEK293 T cells were grown in 15-cm culture dishes in medium with 10% FBS in a humidified atmosphere consisting of 5% CO_2 at 37 °C. The confluent cells were transfected with the WT KOR — pcDNA3.1(+) FLAG-KOR-His_6 (25 μg/15-cm dish), using Fugene 6 transfection reagent (Roche). It contains an N-terminal FLAG tag and a C-terminal His_6 tag. Another Flp-in CHO cell line (Invitrogen), stably expressing hKOR without any epitope tag, was used for studying the washing-resistant RB-64 labeling. The expression of KOR in these cells had been characterized by various radioligand binding and western blotting assays. The affinity constants (K_i) of the different compounds were determined in competition binding assays with [^{3}H]U69593 and [^{3}H]diprenorphine. The details have been described in our previous reports (12,13).

Labeling of synthetic KOR peptides

Synthetic peptides were custom prepared by the Tufts University Core Facility and incubated (1 mg/ml) together with RB-64 overnight at 37 °C in PBS, peptides then prepared for MS as previously detailed (24).

Irreversible binding studies

After a total of 48 hours of transfection, cell media was removed and the transfected cells were washed by cold PBS, then the cells were labeled with RB-64 or RB-48 for various time periods (5 min to several h) and concentrations (0.1 nM-30 μM) in ice-cold PBS. Cells were detached

and centrifuged. Cell pellets were then extensively washed with standard binding buffer, centrifuged at 15,000 *g* for 20 min at 4 °C and prepared for subsequent radioligand binding.

Mass Spectrometric Analysis

MS and MS/MS studies on the labeled synthetic peptide (Tufts University Core Facility) were performed on an Applied Biosystems 4800 Proteomics Analyzer (MALDI-TOF/TOF), using CHCA as matrix.

Prepulse Inhibition Animal Study

Adult naïve male and female C57BL/6J mice (Jackson Labs, Bar Harbor, ME) were used in all experiments. Animals were maintained under a 14:10 h light/dark cycle in a humidity and temperature-controlled room with water and laboratory chow supplied. All experiments were conducted in accordance with NIH guidelines and under an approved protocol from the Institutional Animal Care and Use Committee at Duke University and the University of North Carolina.

Salvinorin A and RB-64 Disrupt Prepulse Inhibition (PPI) in C57BL/6J Mice—

Mice were administered vehicle (1% Tween 80 in Milli-Q water; 8 ml/kg, i.p.) or one of four doses of salvinorin A (0.25, 0.5, 1.0, 2.0 mg/kg, i.p.) or RB-64 (0.005, 0.01, 0.05, 0.1 mg/kg, i.p.) immediately before placement into the PPI apparatus (Med-Associates). In antagonist control studies, mice were administered 10mg/kg *nor*-binaltorphimine (Nor-BNI) i.p., a long-acting selective KOR antagonist, 24h prior to administration of 2.0 mg/kg salvinorin-A or 0.1 mg/kg RB-64 (n=6). After 5 min acclimatization to 62-dB white-noise, animals were administered 84 test trials, beginning and ending with 10 trials each of startle-only stimuli (40 msec 120-dB white-noise burst). The remaining 64 trials were randomized between the following trial types: 8 startle-only trails, 8 trials without any stimuli (null trials), 16 trials with prepulse stimuli (4, 8, 12, and 16 dB above the 62-dB background, 4 of each intensity, 20 msec in length) that were not paired with startle stimuli (prepulse-only trials), and 32 trials of prepulse stimuli (4, 8, 12, and 16 dB above the 62-dB background, 8 at each intensity) paired with the 120 dB startle stimulus given 100 msec following the onset of the prepulse stimulus. Trials were separated by a variable interval (8–15 10sec) and total test-time lasted 26–30 min for each animal. The data were analyzed with SPSS 11 programs (SPSS Inc.) and are presented as means ± standard error of the mean. Differences in treatment effects on null activity, baseline startle responses, and overall PPI were analyzed with ANOVA, with the main effects of dose nested within compound. Repeated measures ANOVA (RMANOVA) was used to examine the effects of salvinorin A and RB-64 on prepulse-dependent PPI, with prepulse intensity (4, 8, 12, and 16 dB) as the within subjects effect, and compound and dose as the between subjects effects (dose nested within compound). Differences between treatment groups were determined with Bonferroni corrected pair-wise comparisons. In all cases, $p < 0.05$ was considered statistically significant.

Molecular Modeling

Unless otherwise noted, all molecular modeling procedures were carried out using SYBYL 8.1 (Tripos, L.P., St. Louis, MO) on Irix-based SGI Tezro, SuSE Linux Enterprise Server-based SGI VSS40 or Red Hat Enterprise Linux-based Hewlett-Packard xw9400 workstations. The Ballesteros-Weinstein amino acid residue numbering system (25) is used to identify conserved residue positions within the TM helices, and is given as a superscript following the amino acid identifier, e.g. $C315^{7.38}$.

The construction and refinement of the KOR-salvinorin A interaction model has been previously described (21) (12) (13). The docked RB-64-KOR complex was obtained by modifying the C-22 position of salvinorin A with a thiocyanate group followed by an energy-

minimization procedure (Tripos Force Field; Gasteiger-Hückel charges; distance-dependent dielectric constant ε=4.0; termination criterion: energy gradient < 0.05 kcal/(mol·Å)). The +431 and +463 salvinorin A-labeled KOR models were constructed by manually joining the docked salvinorin A C-22 carbon atom to the KOR C315$^{7.38}$ S$^{\gamma}$ sulfur atom with the appropriate linker, as these moieties were in close proximity to one another (Figure 1B). This was followed by energy-minimization as described above. The +431 and +463 salvinorin A-labeled F314$^{7.37}$C-C315$^{7.38}$S KOR mutant models were obtained by mutating F314$^{7.37}$ and C315$^{7.38}$ to cysteine and serine, respectively. This was followed by a clockwise rotation (when viewed from the extracellular side) of residues L309$^{7.32}$ to A317$^{7.40}$ by 100° to position C314$^{7.37}$ in the region of space previously occupied by C315$^{7.38}$. The interfacial regions between the rotated TM7 segment and the unrotated parent KOR structure (T302^{EL3} to L309$^{7.32}$ and A317$^{7.40}$ to S323$^{7.46}$) were then remodeled using loop searches. This was followed by repositioning of the sidechains in the rotated segment using SCWRL 3.0 (26). Finally, the ligand was covalently bound to C314$^{7.37}$ as described above for the wt KOR and energy-minimized. The stereochemical quality of the models were assessed using PROCHECK (27) and the ProTable facility within SYBYL to verify that the modifications did not abnormally distort the receptor structure.

RESULTS

Design and synthesis of extraordinarily potent, selective and potentially irreversible ligands for the κ-opioid receptor

Our previously-reported (21) activated KOR-salvinorin A model (Figure 1A) showed C315$^{7.38}$ to be accessible from within the binding pocket and relatively close to the C-2 acetyl group of salvinorin A. In this model, the C-2 acetyl group (C-22 carbon atom) engages in van der Waals interactions with the aromatic sidechain of Y313$^{7.36}$, an interaction that has been suggested (12) (13) to be an important contributor to the unusually high binding affinity and efficacy of salvinorin A. By modifying the conformation of the C-2 acetyl group and switching the C315$^{7.38}$ sidechain rotameric state from *gauche*– to *gauche*+, the C-22 carbon and C315$^{7.38}$ S$^{\gamma}$ sulfur atoms may be brought to within 5 Å of one another (Figure 1B). This arrangement also allows a small substituent at C-22; the electrophilic thiocyanate derivative RB-64 is shown in Figure 1B.

Experimental evidence obtained using the substituted cysteine accessibility method (SCAM) by Xu, et al. (22,28) and us (21) suggests that there is significant rotational flexibility in the extracellular regions of both TM6 and TM7 about their helical axes. Helical rotations are also thought to be important for GPCR activation (see (29) for a current review) and are most likely a property of transmembrane helices in general, especially those containing proline (30) and/or glycine (31). This rotational flexibility should facilitate nucleophilic attack by the C315$^{7.38}$ thiol at either C-22 or an adjacent electrophilic site without requiring significant re-orientation of the ligand. For RB-64, the resulting labeled KOR receptor models result in either a thioether (+431 label; substitution of thiocyanato group) or a disulfide (+463 label; substitution of cyano group) linkage as shown in Figure 1C.

Modeling of the +431- and +463-labeled wt KOR resulted in ligand-receptor complexes whose conformation was minimally perturbed compared to the unlabeled salvinorin A-KOR complex (Figures 2A and 2B.) The change in position of the salvinorin A heavy atoms (not including the C-2 substituent) was 0.63 Å for the +431 label and 0.52 Å for the +463 label (Figure 2A). A similarly small displacement of the KOR backbone in the region of C315$^{7.38}$ was also noted. These results suggest that salvinorin A analogs substituted with electrophilic groups at C-22 would be effective and selective affinity labels for the KOR. Based on these considerations, several salvinorin A derivatives substituted at the C-22 position were synthesized and pharmacologically characterized. Of these, several emerged as potent KOR ligands (Table 1)

with the agonist 22-thiocyanatosalvinorin A (RB-64) demonstrating the highest affinity (0.59 nM). 22-Thiocyanatosalvinorin A also emerged as a sub-nM efficacy agonist in [^{35}S]GTPγS binding assays. To our knowledge RB-64 represents ***the most potent KOR agonist thus far identified***. No significant activity (Ki's>>10,000 nM) at μ- or δ-opioid receptors was revealed for these compounds (not shown).

22-Thiocynatosalvinorin A Wash-resistant Irreversible-binding and Mutagenesis Studies of KOR

Because 22-thiocyanatosalvinorin A and 22-chlorosalvinorin A were predicted to be irreversible inhibitors based on molecular modeling considerations, we next determined if prolonged incubations with either compound led to washing-resistant inhibition of binding. In preliminary studies we found incubation at 4 °C with either 22-thiocyanatosalvinorin A or chlorosalvinorin A resulted in wash-resistant inhibition of binding but that 22-thiocyanatosalvinorin A's were more robust (not shown). A time course and dose-response study of 22-thiocyanatosalvinorin A disclosed a $t_{1/2}$ = 0.4 h and EC_{50} = 9 μM for wash-resistant inhibition of binding (Figures 3A and 3B) at 4 °C. Under these conditions radioligand binding was diminished although there was no change in total KOR protein as assessed by Western blot analysis (not shown). For further experiments, the conditions were chosen (3 h/10 μM at 4 °C in PBS buffer) which gave highly reproducible wash-resistant inhibition of binding. At these conditions, a maximum of 59 % of the KOR could be labeled by 22-thiocyanatosalvinorin A (Figure 3C). For controls, identical incubations with either salvinorin A or naloxone did not substantially alter radioligand binding. Longer incubation times with higher concentrations of 22-thiocyanatosalvinorin A (*e.g.*, 10 h/20 μM) achieved 82% wash-resistant inhibition of KOR binding (not shown). Other high affinity ligands (e.g. 22-bromosalvinorin A) were also tested as potential affinity ligands although none showed significant irreversible inhibition of binding.

As indicated previously, molecular modeling studies predicted that 22-thiocyanatosalvinorin A would interact with C315$^{7.38}$. Accordingly the C315$^{7.38}$S single and F314$^{7.37}$C(C315$^{7.38}$S) double mutants were tested for wash-resistant inhibition of binding (Figure 3D). As expected C315$^{7.38}$S did not show any apparant reactivity with 22-thiocyanatosalvinorin A as compared to naloxone. Significantly, F314$^{7.37}$C(C315$^{7.38}$S), which is predicted to introduce a free thiol in the vicinity of the thiocyanato group, produced significant apparant reactivity.

In the wt KOR-salvinorin A complex (Figure 1A), the F314$^{7.37}$ side chain is oriented away from the binding pocket. However, the putative rotational flexibility of the extracellular region of TM7 mentioned above allows position 7.37 to be accessed by a ligand from within the binding cavity. In many of the experimentally-determined GPCR structures to date, TM7 contains an 'overwound' section of 3_{10}-helix at positions 7.41 to 7.46 followed by a conserved proline-induced kink at 7.46 to 7.48. Residues on TM7 following position 7.48 (in the intracellular region) are involved in an H-bonding network ('NPxxY') that is highly conserved among rhodopsin-like GPCRs. Thus, one possible explanation for the observed pattern of enhanced accessibility (21) of the residues in the TM7 extracellular region is that this overwound section can become 'unwound', resulting in an α- or π-helical geometry and a corresponding clockwise rotation of the extracellular portion of TM7 (as viewed from the extracellular side). The amount of rotation needed to make position 7.37 ligand-accessible is roughly 100° (3.6 residues per turn in a regular α-helix = 100° per residue), which will introduce a bulge similar to the conserved π-bulge observed in TM5 of rhodopsin-like GPCRs (32). Such 'wide turn' regions are known to impart flexibility to transmembrane-spanning helices (33). In the KOR, the overwound region also contains a glycine residue G319$^{7.42}$ that will tend to increase the local flexibility of the backbone due to the absence of a sidechain and further promote the rotation of the extracellular region of TM7. RB64-labeled F314$^{7.37}$C-C315$^{7.38}$S

double-mutant KOR models were generated with these concepts in mind, and are shown in Figures 2B and 2C.

Identification of a potential mechanism for irreversible inhibition of binding using model peptide substrates

Covalently-bound ligands can label the cysteine residue through different chemical pathways. To explore the possible reaction pathways, a synthetic model peptide (Ac-YFCIALGY) was used to mimic the covalent-labeling between RB-64 and KOR protein. A parallel mass spectrometric examination of RB-64, RB-48 and salvinorin A revealed the possible fragmentation mechanisms of the parent compounds (Figures 4A and 4B). All of the major product ions were assigned, including m/z 378, 373, 355 and 350 and our control observations for salvinorin A are in excellent agreement with prior studies (34) (35) while the results with RB-64 and RB-48 are new.

After incubating RB-64 with the model peptide at 37 °C overnight, one major product (m/z 1475) was identified in MS (Figure 5B). This indicated that free-peptide labeling preferred nucleophilic substitution of the cyano group with the formation of a disulfide bond as shown in Figure 1C. This new pathway was confirmed by the MS/MS analysis of m/z 1475 (Figure 5C).

22-thiocyanatosalvinorin A is extraordinarily potent in vivo

Prepulse inhibition (PPI) is a measure of sensory motor gating (36) (37) (38) and a large number of studies have validated disruption of PPI as an indicator of potential psychotimimetic properties. Because salvinorin A is the most potent naturally-occurring hallucinogen (5), we predicted that both 22-thiocyanatosalvinorin A and salvinorin A have effects on PPI. We observed an extraordinarily high potency of RB-64 as compared to salvinorin A. Salvinorin A and RB-64 produced changes in activity during null trails (without any stimuli) compared to vehicle-treated mice (Supplementary Table 1). Mice treated with salvinorin A showed significant increases in null activity with 0.5 mg/kg ($p < 0.001$) compared to all other doses of the compound and the vehicle controls. Effects of RB-64 were somewhat different. The two lower doses of RB-64 had little effect on null activity, whereas the two highest doses resulted in increased activity compared to the vehicle control ($p < 0.001$).

Mice treated with salvinorin A or RB-64 showed dose-dependent parabolic changes in baseline startle activity (Figure 6A). Overall PPI was affected by salvinorin A (Figure 6B) and 22-thiocyanatosalvinorin A (Figure 6C). Bonferroni corrected pair-wise comparisons found that overall inhibition was similar for vehicle and 0.25, 0.5, or 1 mg/kg salvinorin A, while 2 mg/kg significantly suppressed inhibition ($p < 0.044$). By comparison, 0.01 and 0.05 mg/kg RB-64 resulted in marked increases in overall inhibition compared to the vehicle control ($p < 0.021$). Mice given 0.1 mg/kg RB-64 showed a significant reduction in overall inhibition relative to vehicle-treated mice ($p < 0.046$). Mice treated with vehicle showed prepulse-dependent PPI. Salvinorin A or RB-64 disrupted prepulse-dependent PPI at all prepulse intensities. Mice given 0.25, 0.5 or 1 mg/kg salvinorin A had increased PPI to the 4-dB prepulse, relative to vehicle ($p < 0.051$) (Figure 6B); PPI responses at the 8- and 12-dB prepulses were similar for animals administered vehicle, or 0.25, 0.5, or 1 mg/kg salvinorin A. However, mice given 2 mg/kg salvinorin A had marked reductions in PPI at the 8-, 12-, and 16-dB prepulses compared to vehicle ($p > 0.011$) or all other doses of the compound ($p < 0.047$); responses to 4 dB were unchanged from the vehicle control. When animals were given 0.005, 0.01, or 0.05 mg/kg RB-64, PPI to the 4 dB prepulse were enhanced relative to vehicle ($p < 0.047$) (Figure 6C). By comparison, 0.005 RB-64 depressed responses to the 12- and 16-dB prepulses ($p < 0.010$). The 0.01 and 0.05 doses increased PPI to the 8-dB prepulse relative to the vehicle controls ($p < 0.031$). Similarly, 0.05 mg/kg RB-64 increased the responses to the 12- and 16-db prepulses

($p < 0.052$). Responses to the highest doses of RB-64 were different than those for the 0.01 and 0.05 doses. Here, responses to the 12- and 16-dB prepulses were significantly depressed compared to the vehicle control ($p < 0.003$). In antagonist control studies, mice were administered the selective KOR antagonist *nor*-binaltorphimine (Nor-BNI) (10mg/kg) prior to administration of 2.0 mg/kg salvinorin-A or 0.1 mg/kg RB-64 (Figures 6D and 6E). Nor-BNI antagonized salvinorin A and RB-64-induced disruption of PPI, indicating the behavioral responses of both compounds are mediated by KOR.

DISCUSSION

In this paper we report the successful modeling-based design, synthesis and pharmacological characterization of novel salvinorin A-derived KOR affinity ligands. Diffusible ligands bind to receptors mainly through non-covalent interactions, such as electrostatic forces, hydrogen bonds, van der Waals' forces and hydrophobic effects. In contrast, affinity ligands can directly link to the receptor protein, and thus can present with unique biophysical and pharmacological properties. As is evident, RB-64 displays high affinity, potency, and selectivity for KOR (Table 1), and this indicates that affinity ligands can significantly improve the efficacy and selectivity for their corresponding receptors without the introduction of off-target effects. As an apparent affinity ligand, RB-64 shows great potential as a molecular probe to explore κ-opioid receptor structure and function. To our knowledge, RB-64 represents the first selective agonist affinity ligand for KORs. These studies also provide the first direct evidence for a reactive cysteine in the binding pocket of KOR in support of many prior modeling and biochemical studies.

Based on our previous binding site model (21) (12) (13), the C-2 position of salvinorin A is in close proximity to $Y313^{7.38}$, so that residues $C315^{7.36}$ and $F314^{7.37}$ are in a favorable position for covalent labeling. Our rational design of affinity ligands based on the structure of salvinorin A further confirmed the proposed binding mode interaction between KOR and salvinorin A. Interestingly, in the labeling experiment, RB-64 can undergo two different chemical reaction pathways (Figure 1C). In a restricted biological environment, such as the binding pocket of KOR, multiple factors (*e.g.*, ligand orientation, space restriction, etc.) will not allow all of the possible chemical reactions to occur. Indeed, the mass spectrometric analysis of the short synthetic peptide (YFCIALGY) revealed a substitution of the cyano group and in future studies it will be important to determine if this reaction mode is conserved in the intact KOR.

These studies are significant because they clearly demonstrate that the modeling-based synthesis of affinity ligands can be highly successful. Our ability to predict the orientation and mode of binding of the various salvinorin A derivatives we prepared was highly dependent on prior studies in which we applied a variety of approaches including molecular modeling, directed mutagenesis, substituted cysteine-accessibility mutagenesis, and salvinorin A analogue synthesis to arrive at a testable model of agonist binding to the KOR.

Our synthetic design of salvinorin A-derived irreversible affinity labels assumed the introduction of electron-withdrawing groups at C-22 in order to increase the electrophilicity of this center and make it capable of forming a covalent bond with SH-group of C315. We selected halogen atoms (e.g. chlorine, bromine) for this purpose due to their good leaving group character for nucleophilic substitution with thiols. Several salvinorin A derivatives having one or two chlorine atoms at C-22 were synthesized (see Table 1). In this group of compounds the 22-bromo- and 22-chlorosalvinorin (RB-48) were comparable to salvinorin A in KOR binding affinity. Interestingly, replacement of the chlorine atom with an electron-donating methoxy group only slightly lowered the affinity. Finally, introduction of a thiocyanate group via a simple reaction with potassium thiocyanate afforded us a ligand which apparently covalently bound to KOR and activated the receptor with exceptionally high potency. The difference between the binding affinity at room temperature with purified membranes (39 nM at ^{3}H-

diprenorphine-labelled KOR) and the EC_{50} for apparent irreversible labeling in intact cells (1200 nM) is commonly seen with affinity ligands and has been previously reported with opioid affinity ligands (39) (40,41,42).

The thiocyanate group is not commonly used in affinity labeling. Indeed, only a few futile attempts of using this group are known. Much more commonly used isothiocyanates provided good labels in forming covalent bonds with free amino group of proteins in addition rather than substitution reactions. Reaction of isothiocyanates with cysteine residues, although known, are much less common. Another advantage of thiocyanato derivatives over isothiocyanates is the simplicity of the synthesis from corresponding chloro derivatives. 22-Thiocyantosalvinorin (RB-64) is a solid and stable compound and may be stored for prolonged time without decomposition. Finally, it is evident that thiocynatosalvinorin (RB-64) is considerably more potent than salvinorin A at disrupting sensory-motor gating *in vivo* and these results are in good agreement with its enhanced agonist potency *in vitro*.

In conclusion, we describe the first successful model-based design and synthesis of agonist affinity ligands for KOR—thiocynatosalvinorin (RB-64). We also provide a reasonable model describing RB-64's mode of interaction with KOR via mutagenesis studies and high resolution proteomics studies of model KOR membrane protein synthetic peptides. These studies provide the first direct evidence for the presence of a free cysteine in the agonist-bound state of KOR and provide novel insights into the mechanism by which salvinorin A and its analogues bind to and activate KOR.

Abbreviations

GPCR, G protein-coupled receptor
KOR, κ-opioid receptor
hKOR, human KOR
Gα, G protein alpha subunit
TM, transmembrane domain
CHCA, α-cyano-4-hydroxycinnamic acid
CID, collision-induced dissociation
EL, extracellular loop
IL, intracellular loop
MALDI, matrix assisted laser desorption/ionization
MS, mass spectrometry
MS/MS, tandem mass spectrometry, m/z, mass to charge ratio
S/N, signal to noise ratio
TOF, time of flight
b_n and y_n, Bieman-modified Roepstorff and Fohlman peptide ion nomenclature.

Acknowledgments

We thank Drs. Vernon E. Anderson, Martin D. Snider, Paul R. Ernsberger and Krzysztof Palczewski for comments and suggestions on the manuscript. The pcDNA3.1(+) FLAG-KOR-His_6 vector was made by Dr. Timothy A. Vortherms. The Flp-In CHO cell line (Invitrogen) stably expressing hKOR was made by Joe Rittiner. JKZ thanks Lukasz Kutrzeba for his help with NMR measurements. Mass spectrometers were provided by both the Department of Pharmacology of UNC, Chapel Hill and the UNC-Duke Proteomics Center, which was partially funded by a gift from an anonymous donor.

REFERENCES

1. Ortega A, Blount JF, Manchand PS. Salvinorin: a new *trans*-neoclerodane diterpene from *Salvia divinorum* (Labiatae). J Chem Soc Perkins Trans I 1982:2505–2508.

2. Valdes LJ, Butler WM, Hatfield GM, Paul AG, Koreeda M. Divinorin A: a psychotropic terpenoid and divnorin B from the hallucinogenic Mexican mint Salvia divinorum. J Org Chem 1984;49:4716–7720.
3. Roth BL, Baner K, Westkaemper R, Siebert D, Rice KC, Steinberg S, Ernsberger P, Rothman RB. Salvinorin A: a potent naturally occurring nonnitrogenous kappa opioid selective agonist. Proc Natl Acad Sci U S A 2002;99:11934–11939. [PubMed: 12192085]
4. Ansonoff MA, Zhang J, Czyzyk T, Rothman RB, Stewart J, Xu H, Zjwiony J, Siebert DJ, Yang F, Roth BL, Pintar JE. Antinociceptive and hypothermic effects of Salvinorin A are abolished in a novel strain of kappa-opioid receptor-1 knockout mice. J Pharmacol Exp Ther 2006;318:641–648. [PubMed: 16672569]
5. Sheffler DJ, Roth BL. Salvinorin A: the "magic mint" hallucinogen finds a molecular target in the kappa opioid receptor. Trends Pharmacol Sci 2003;24:107–109. [PubMed: 12628350]
6. Vortherms TA, Roth BL. Salvinorin A: from natural product to human therapeutics. Mol Interv 2006;6:257–265. [PubMed: 17035666]
7. Harding WW, Tidgewell K, Byrd N, Cobb H, Dersch CM, Butelman ER, Rothman RB, Prisinzano TE. Neoclerodane diterpenes as a novel scaffold for mu opioid receptor ligands. J Med Chem 2005;48:4765–4771. [PubMed: 16033256]
8. Harding WW, Schmidt M, Tidgewell K, Kannan P, Holden KG, Dersch CM, Rothman RB, Prisinzano TE. Synthetic studies of neoclerodane diterpenes from Salvia divinorum: selective modification of the furan ring. Bioorg Med Chem Lett 2006;16:3170–3174. [PubMed: 16621556]
9. Groer CE, Tidgewell K, Moyer RA, Harding WW, Rothman RB, Prisinzano TE, Bohn LM. An opioid agonist that does not induce micro-opioid receptor--arrestin interactions or receptor internalization. Mol Pharmacol 2007;71:549–557. [PubMed: 17090705]
10. Simpson DS, Katavic PL, Lozama A, Harding WW, Parrish D, Deschamps JR, Dersch CM, Partilla JS, Rothman RB, Navarro H, Prisinzano TE. Synthetic Studies of Neoclerodane Diterpenes from Salvia divinorum: Preparation and Opioid Receptor Activity of Salvinicin Analogues. J Med Chem 2007;50:3596–3603. [PubMed: 17580847]
11. Prisinzano TE, Rothman RB. Salvinorin A analogs as probes in opioid pharmacology. Chem Rev 2008;108:1732–1743. [PubMed: 18476672]
12. Yan F, Mosier PD, Westkaemper RB, Stewart J, Zjawiony JK, Vortherms TA, Sheffler DJ, Roth BL. Identification of the molecular mechanisms by which the diterpenoid salvinorin A binds to kappa-opioid receptors. Biochemistry 2005;44:8643–8651. [PubMed: 15952771]
13. Vortherms TA, Mosier PD, Westkaemper RB, Roth BL. Differential helical orientations among related G protein-coupled receptors provide a novel mechanism for selectivity. Studies with salvinorin A and the kappa-opioid receptor. J Biol Chem 2007;282:3146–3156. [PubMed: 17121830]
14. Tan KR, Gonthier A, Baur R, Ernst M, Goeldner M, Sigel E. Proximity-accelerated chemical coupling reaction in the benzodiazepine-binding site of gamma-aminobutyric acid type A receptors: superposition of different allosteric modulators. J Biol Chem 2007;282:26316–26325. [PubMed: 17626010]
15. Luo Y, Knuckley B, Bhatia M, Pellechia PJ, Thompson PR. Activity-based protein profiling reagents for protein arginine deiminase 4 (PAD4): synthesis and in vitro evaluation of a fluorescently labeled probe. J Am Chem Soc 2006;128:14468–14469. [PubMed: 17090024]
16. Cohen MS, Zhang C, Shokat KM, Taunton J. Structural bioinformatics-based design of selective, irreversible kinase inhibitors. Science 2005;308:1318–1321. [PubMed: 15919995]
17. Cohen MS, Hadjivassiliou H, Taunton J. A clickable inhibitor reveals context-dependent autoactivation of p90 RSK. Nat Chem Biol 2007;3:156–160. [PubMed: 17259979]
18. Mattras H, Aliau S, Demey E, Poncet J, Borgna JL. Mass spectrometry identification of covalent attachment sites of two related estrogenic ligands on human estrogen receptor alpha. J Steroid Biochem Mol Biol 2006;98:236–247. [PubMed: 16513342]
19. Mattras H, Aliau S, Richard E, Bonnafous JC, Jouin P, Borgna JL. Identification by MALDI-TOF mass spectrometry of 17 alpha-bromoacetamidopropylestradiol covalent attachment sites on estrogen receptor alpha. Biochemistry 2002;41:15713–15727. [PubMed: 12501200]
20. Foucaud B, Alarcon K, Sakr E, Goeldner M. Binding-site chemical probing in homology models using affinity labeling of cysteine-substituted receptors. Curr. Chem. Biol 2007;1:271–277.

21. Yan F, Mosier PD, Westkaemper RB, Roth BL. Galpha-Subunits Differentially Alter the Conformation and Agonist Affinity of kappa-Opioid Receptors. Biochemistry 2008;47:1567–1578. [PubMed: 18205395]
22. Xu W, Chen C, Huang P, Li J, de Riel JK, Javitch JA, Liu-Chen LY. The conserved cysteine 7.38 residue is differentially accessible in the binding-site crevices of the mu, delta, and kappa opioid receptors. Biochemistry 2000;39:13904–13915. [PubMed: 11076532]
23. Xu W, Campillo M, Pardo L, de Riel JK, Liu-Chen L-Y. The Seventh Transmembrane Domains of the δ and κ Opioid Receptors Have Different Accessibility Patterns and Interhelical Interactions. Biochemistry 2005;44:16014–16025. [PubMed: 16331961]
24. Strachan RT, Sheffler DJ, Willard B, Kinter M, Kiselar JG, Roth BL. Ribosomal S6 Kinase 2 Directly Phosphorylates the 5-Hydroxytryptamine 2A (5-HT2A) Serotonin Receptor, Thereby Modulating 5-HT2A Signaling. J Biol Chem 2009;284:5557–5573. [PubMed: 19103592]
25. Ballesteros JA, Weinstein H. Integrated Methods for the Construction of Three-Dimensional Models and Computational Probing of Structure-Function Relations in G Protein-Coupled Receptors. Methods in neurosciences 1995;25:366.
26. Cantescu AA, Shelenkov AA, Dunbrack RL Jr. A Graph-theory Algorithm for Rapid Protein Side-chain Prediction. Protein Sci 2003;12:2001–2014. [PubMed: 12930999]
27. Laskowski RA, MacArthur MW, Moss DS, Thornton JM. PROCHECK: A Program to Check the Stereochemical Quality of Protein Structures. J. Appl. Cryst 1993;26:283–291.
28. Xu W, Campillo M, Pardo L, Kim de Riel J, Liu-Chen LY. The seventh transmembrane domains of the delta and kappa opioid receptors have different accessibility patterns and interhelical interactions. Biochemistry 2005;44:16014–16025. [PubMed: 16331961]
29. Wess J, Han SJ, Kim SK, Jacobson KA, Li JH. Conformational changes involved in G-protein-coupled-receptor activation. Trends Pharmacol Sci 2008;29:616–625. [PubMed: 18838178]
30. Sansom MS, Weinstein H. Hinges, swivels and switches: the role of prolines in signalling via transmembrane alpha-helices. Trends Pharmacol Sci 2000;21:445–451. [PubMed: 11121576]
31. Edwards MD, Li Y, Kim S, Miller S, Bartlett W, Black S, Dennison S, Iscla I, Blount P, Bowie JU, Booth IR. Pivotal role of the glycine-rich TM3 helix in gating the MscS mechanosensitive channel. Nat Struct Mol Biol 2005;12:113–119. [PubMed: 15665866]
32. Ballesteros JA, Jensen AD, Liapakis G, Rasmussen SG, Shi L, Gether U, Javitch JA. Activation of the beta 2-adrenergic receptor involves disruption of an ionic lock between the cytoplasmic ends of transmembrane segments 3 and 6. J Biol Chem 2001;276:29171–29177. [PubMed: 11375997]
33. Riek RP, Finch AA, Begg GE, Graham RM. Wide Turn Diversity in Protein Transmembrane Helices Implications for G-Protein-Coupled Receptor and Other Polytopic Membrane Protein Structure and Function. Mol Pharmacol 2008;73:1092–1104. [PubMed: 18202304]
34. Medana C, Massolino C, Pazzi M, Baiocchi C. Determination of salvinorins and divinatorins in Salvia divinorum leaves by liquid chromatography/multistage mass spectrometry. Rapid Commun Mass Spectrom 2006;20:131–136. [PubMed: 16331747]
35. Barnes S, Prasain JK, Wang CC, Moore DR 2nd. Applications of LC-MS in the study of the uptake, distribution, metabolism and excretion of bioactive polyphenols from dietary supplements. Life Sci 2006;78:2054–2059. [PubMed: 16460766]
36. Ouagazzal A, Grottick AJ, Moreau J, Higgins GA. Effect of LSD on prepulse inhibition and spontaneous behavior in the rat. A pharmacological analysis and comparison between two rat strains. Neuropsychopharmacology 2001;25:565–575. [PubMed: 11557170]
37. Geyer MA, Braff DL. Startle habituation and sensorimotor gating in schizophrenia and related animal models. Schizophr Bull 1987;13:643–668. [PubMed: 3438708]
38. Braff DL, Geyer MA. Acute and chronic LSD effects on rat startle: data supporting an LSD-- rat model of schizophrenia. Biol Psychiatry 1980;15:909–916. [PubMed: 7193055]
39. Manda S, Lerner-Marmarosh N, Hashmi M, Abood LG. Opioid receptor antagonist affinity ligands: 6 beta-bromoacetamido-6-desoxynaltrexone and 6 beta-thioglycolamido-6-desoxynaltrexone. Neurochem Res 1992;17:1191–1194. [PubMed: 1334238]
40. Tam SW, Liu-Chen LY. Reversible and irreversible binding of beta-funaltrexamine to mu, delta and kappa opioid receptors in guinea pig brain membranes. J Pharmacol Exp Ther 1986;239:351–357. [PubMed: 3021954]

41. Tam SW, Nickolson VJ, Liu-Chen LY. [3H]beta-funaltrexamine binds covalently to brain opioid receptors. Eur J Pharmacol 1985;119:259–260. [PubMed: 3004996]

42. Cheng CY, Wu SC, Hsin LW, Tam SW. Selective reversible and irreversible ligands for the kappa opiate receptor. J Med Chem 1992;12:2243–2247. [PubMed: 1319495]

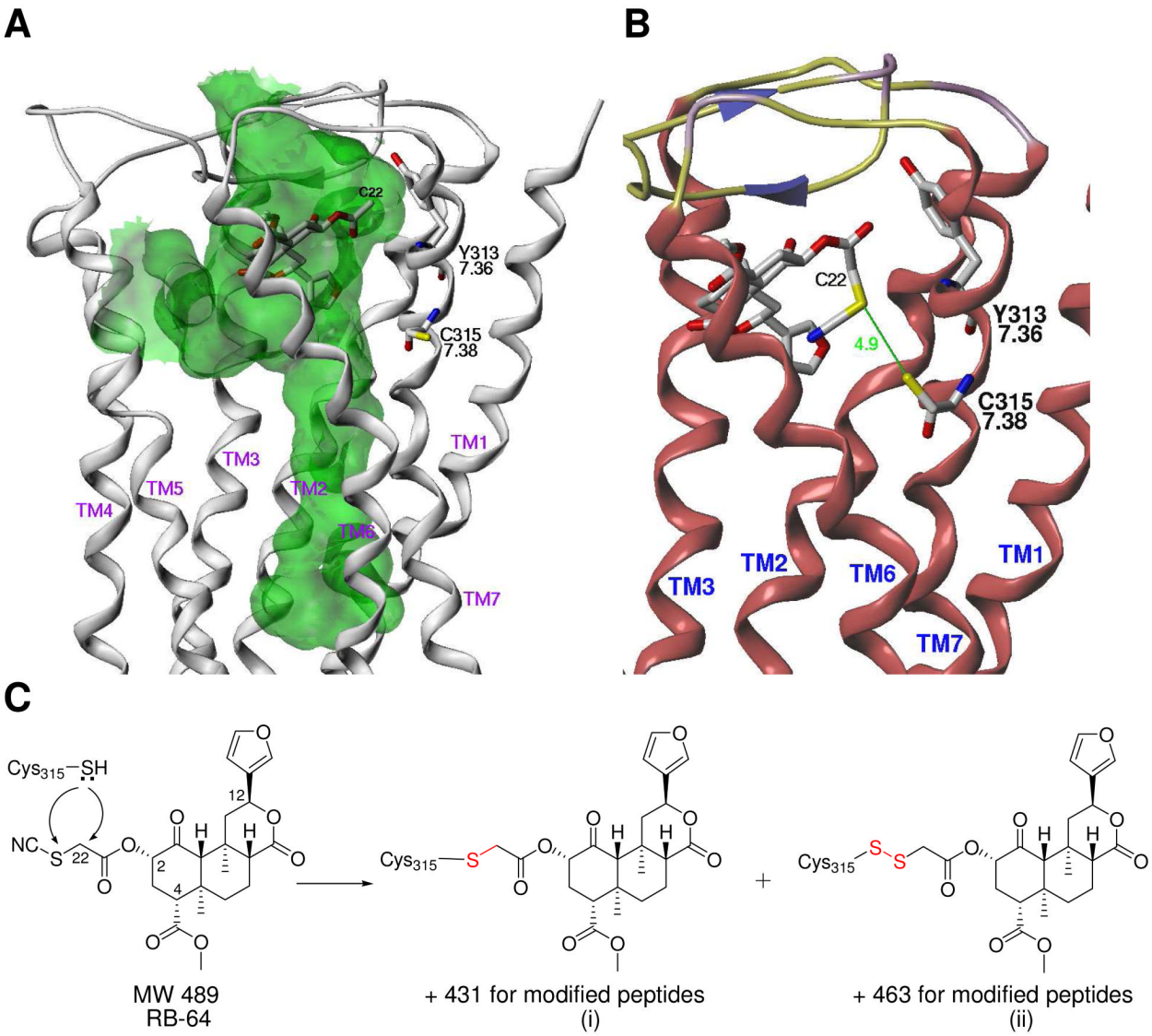

Figure 1. Molecular modeling reveals potential sites of adduct formation at KOR

(A) The C-2 position of salvinorin A is in close proximity to Y313$^{7.36}$ and C315$^{7.38}$ in the wt KOR. Ribbons (white) indicate the position of the backbone, and a Connolly channel surface (green) describes the regions of steric accessibility within the activated receptor. An enlarged region of accessibility in the intracellular portion of the helical bundle is indicative of an activated GPCR. (B) The RB-64 thiocyanate group is in close proximity to C315$^{7.38}$. (C) The mechanisms for covalent-labeling of cysteine involve nucleophilic substitution at C-22 or the adjacent S atom. The molecular weight change for the modified peptides is 431 (i) or 463 (ii) depending on the site of substitution.

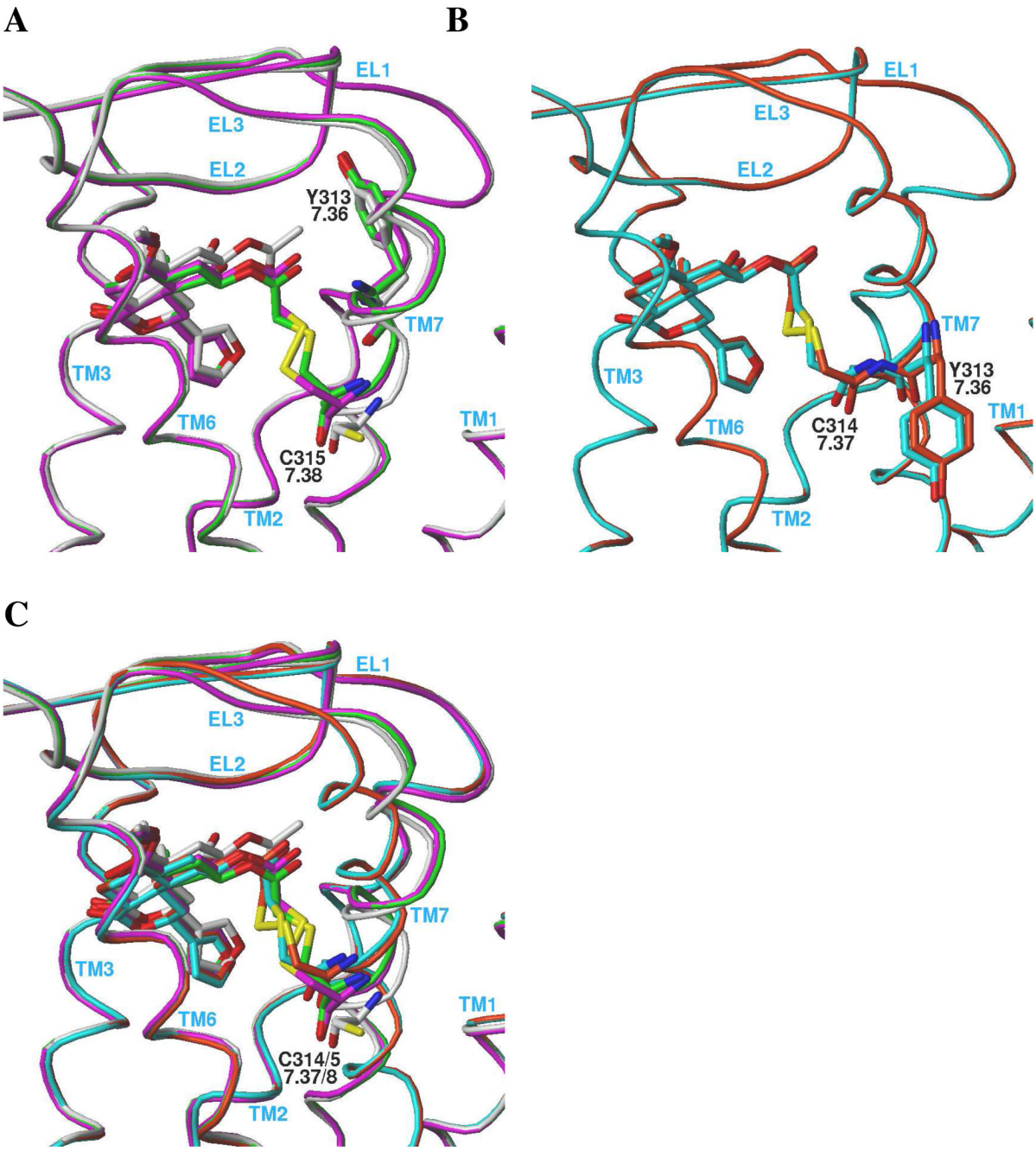

Figure 2. A comparison of the binding modes of Salvinorin A and the +431 and +463 adducts

The color of the backbone ribbons and displayed carbon atoms identify the receptor-ligand complex. A) wt KOR: Salvinorin A (white); +431 adduct (green); +463 adduct (magenta). B) $F314^{7.37}C$-$C315^{7.38}S$ KOR double mutant: +431 adduct (cyan); +463 adduct (orange). C) all receptor-ligand complexes displayed in the same frame of reference. See text for details.

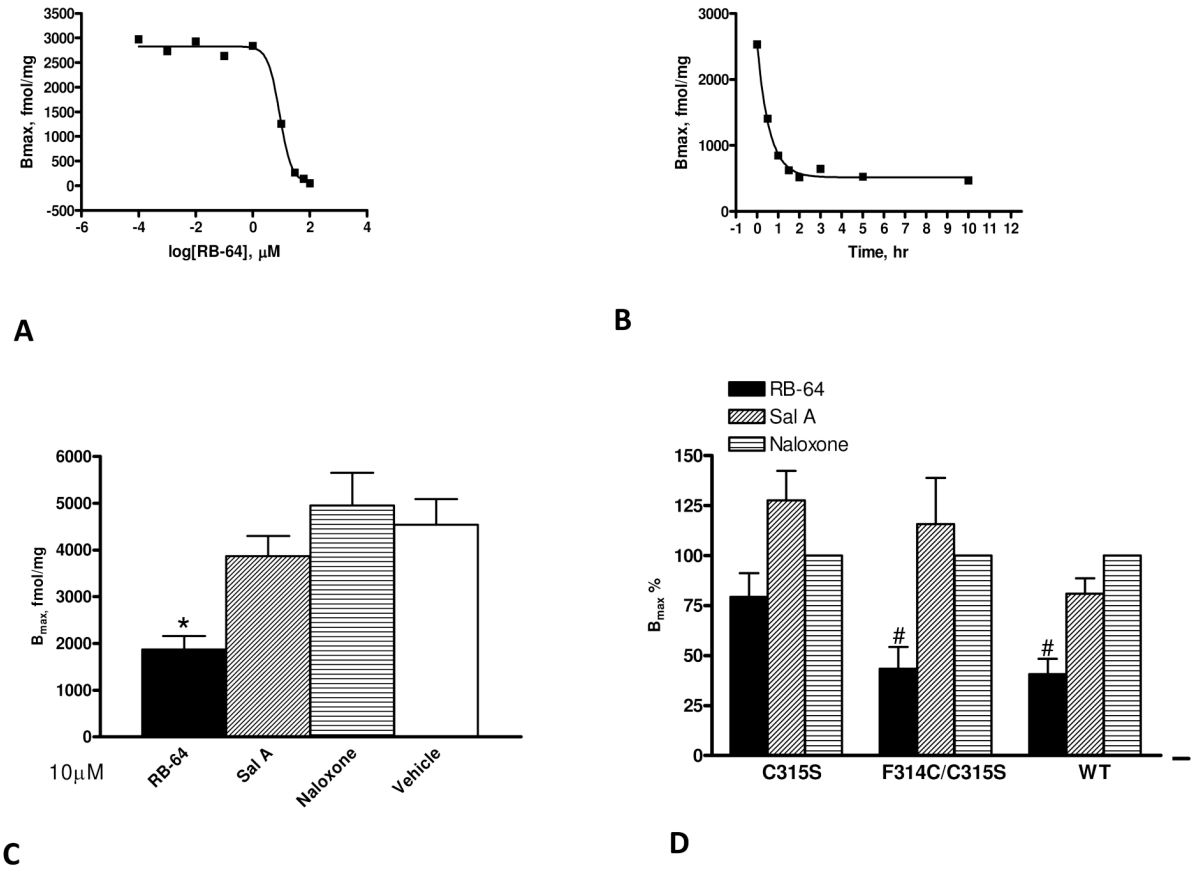

Figure 3. RB-64 induces wash-resistant inhibition of KOR binding at C315

(A) Dose-response curve for RB-64 for wash-resistant inhibition of binding at 4 °C (2 h) yielding an EC_{50} of 1.2 μM. (B) Time-course study at 4 °C with a maximally-effective dose of RB-64 (10 μM) yielding $t_{1/2}$ = 0.4 h. (C) Cells expressing KOR were exposed for 10 μM/3 h to RB-64, salvinorin A, naloxone and vehicle (DMSO only). After incubation, the cell membranes were extensively washed (at least three times); the residual binding was determined by [^{3}H]diprenorphine saturation binding. Data presented are B_{max} values for 2–4 independent experiments. (D) B_{max} values of various mutants after being labeled with RB-64, salvinorin A and naloxone. B_{max} values were expressed as a percentage of vehicle control. Each bar represents the mean ± SEM for two to four independent experiments. An asterisk (*) indicates that RB-64 labeling was significantly different ($p < 0.01$) from the reference (vehicle) by ANOVA. A hash mark (#) indicates that RB-64 labeling was significantly different ($p < 0.05$) than that of naloxone by ANOVA.

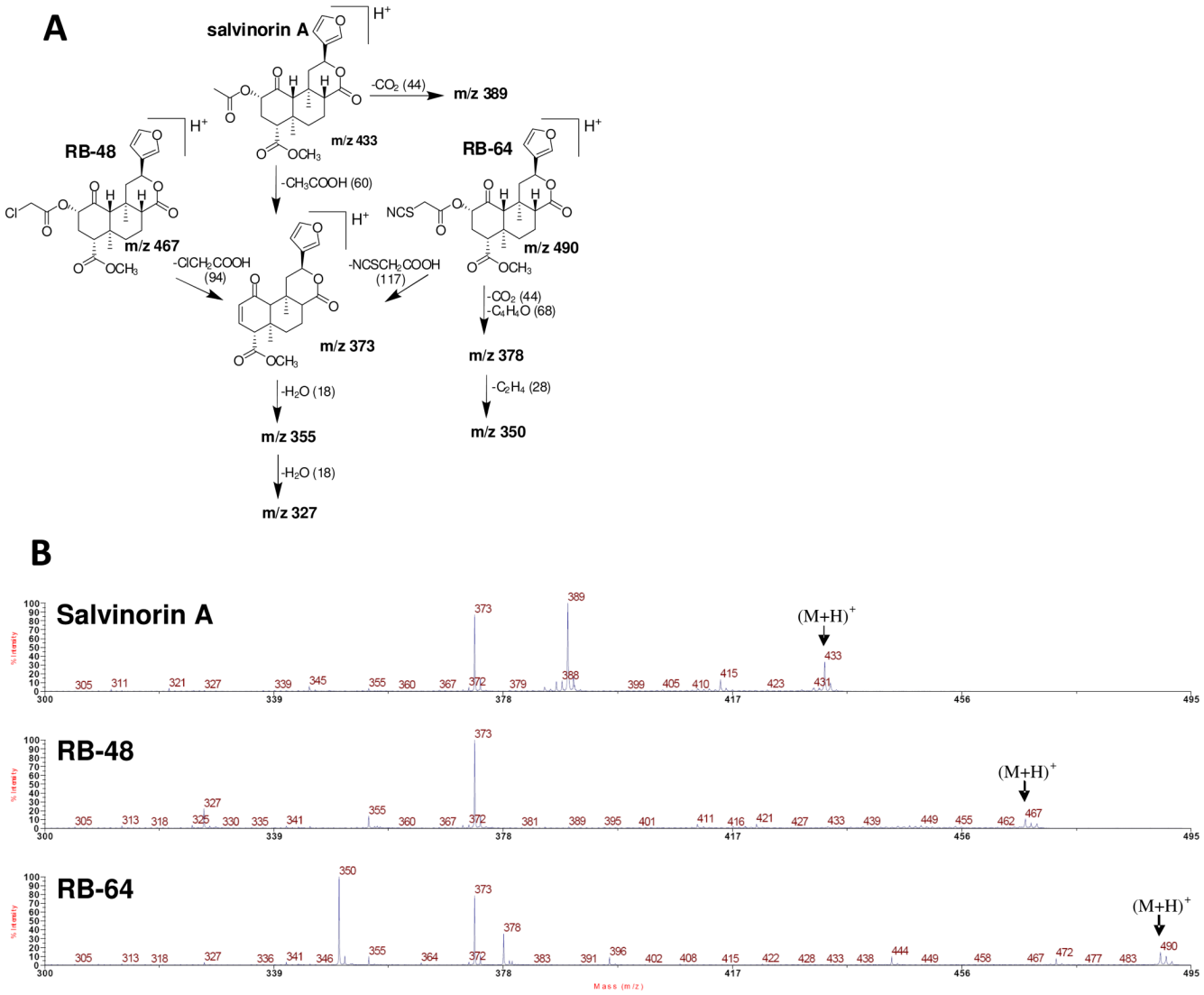

Figure 4. Fragmentation pathways for salvinorin A, RB-48 and RB-64

(A) Deduced structures of the major identified fragments. (B) MS/MS spectra for salvinorin A, RB-48 and RB-64 (from top to bottom), whose precursor ions are 433, 467 and 490 m/z respectively.

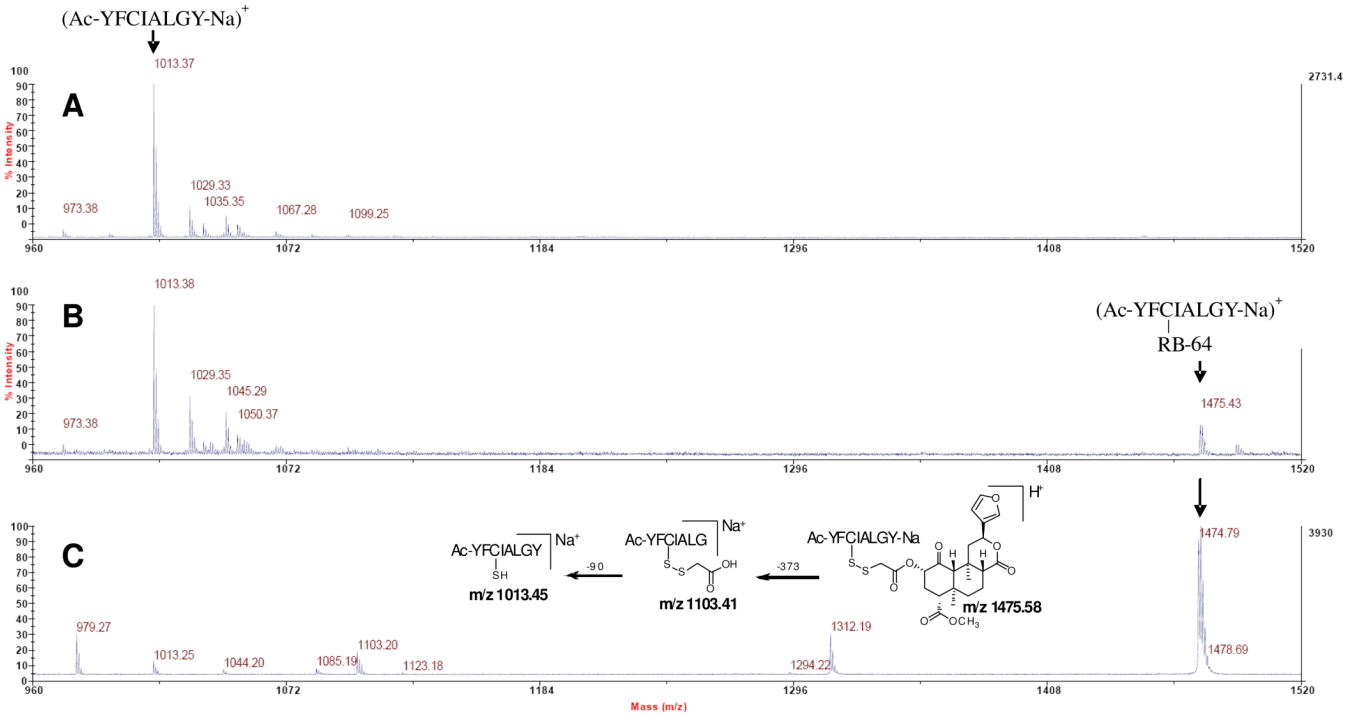

Figure 5. Identification of adduct at C315 via model KOR peptides

The MS spectra of unlabeled (A) and RB-64-labeled (B) peptide Ac-YFCIALGY-Na, MS/MS spectrum with 1475.5 m/z is shown in (C), which contains several major fragments from the RB-64 modified peptide.

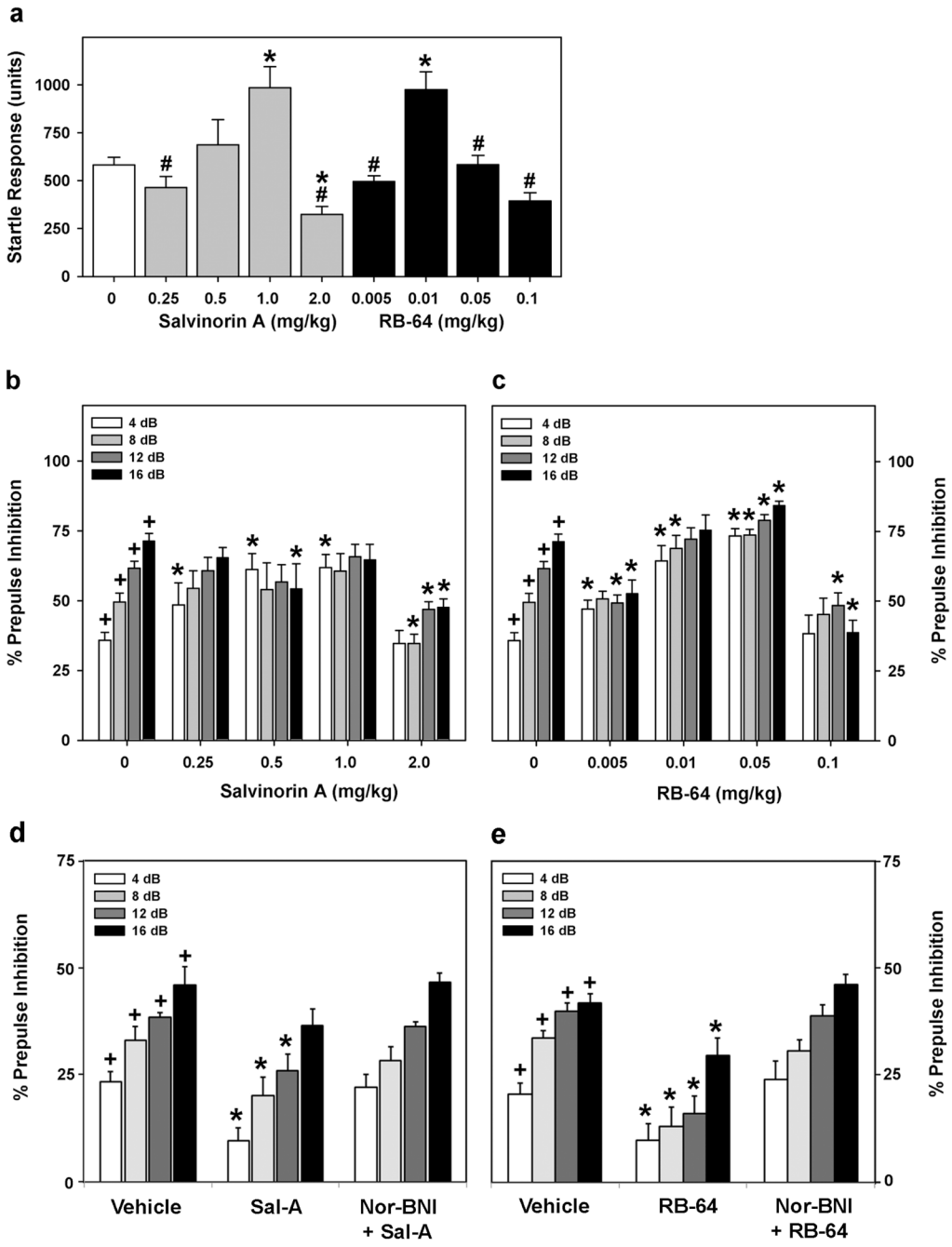

Figure 6. RB-64 is a potent psychotomimetic agent *in vivo*

(A) Startle responses to the 120-db stimulus for animals administered different doses of salvinorin A or RB-64. A hash mark (#) indicates $p < 0.05$ in comparisons of startle responses to 0.5 mg/kg salvinorin A or 0.01 mg/kg RB-64. (B) Percent PPI to the 4-, 8-, 12-, and 16-db prepulses for animals given various doses of salvinorin A. (C) Percent PPI to the 4-, 8-, 12-, and 16-db prepulses for animals given various doses of RB-64. N = 10–16 mice/treatment. (D) Percent PPI to the 4-, 8-, 12-, and 16-db prepulses for animals administered 2 mg/kg salvinorin A or 10mg/kg Nor-BNI followed by 2 mg/kg salvinorin A. N = 6 mice/treatment. (E) Percent PPI to the 4-, 8-, 12-, and 16-db prepulses for animals administered 0.1 mg/kg RB-64 or 10mg/kg Nor-BNI followed by 0.1 mg/kg RB-64. N = 6 mice/treatment. An asterisk (*) indicates *p*

< 0.05 compared to vehicle controls; a plus sign (+) indicates $p < 0.05$ in comparisons of prepulse-dependent PPI at the 4-, 8-, 12-, and 16-dB prepulses within a single treatment.

Table 1

The pharmacological profiles of salvinorin derivatives substituted at C-22.

	K_i[a], nM	K_i[b], nM	EC_{50}[c], nM	*Relative* E_{max}
Salvinorin A	1.8 ± 1.4	21 ± 11	17 ± 6	100%
22-Chlorosalvinorin A (RB-48)	2.1 ± 0.8[d]	32 ± 15	0.19 ± 0.01	85 ± 3%
22-Thiocyanatosalvinorin A (RB-64)	0.59 ± 0.21	39 ± 11	0.077 ± 0.016	95 ± 2%
22-Bromosalvinorin A (RB-50)	1.5 ± 0.22	39.57 ± 11.56	11 +/− 6	76 +/− 7%
(22-*R*,*S*)-22-Chloro-22-methylsalvinorin A (RB-55)	21 ±3	189 ± 70.12	35 +/− 17	83 +/− 10%
(22-*S*)-22-Chloro-22-methylsalvinorin A (RB-55-1)	30 ± 15	269 ± 48	160 +/− 80	99 +/− 12%
(22-*R*)-22-Chloro-22-methylsalvinorin A (RB-55-2)	58 ± 32	>3000	273 +/− 130	98 +/− 8%
22-Methoxysalvinorin A (RB-65)	5.7 ± 1.2	431.3 ± 54.13	67 +/− 22	99 +/− 11%
22,22-Dichlorosalvinorin A (RB-66)	911 ± 170	>10,000	1678 +/− 320	103 +/− 14%

[a] The affinity constants (K_i) of the different compounds were determined in competition binding assays with [^{3}H]U69593 and increasing concentrations of unlabeled compounds. Each value is the mean of three independent experiments.

[b] The affinity constants (K_i) of the different compounds were determined in competition binding assays with [^{3}H]diprenorphine.

[c] The functional potency (EC_{50}) of the different compounds were determined with an [^{35}S]GTPγS assay.

[d] RB-48 showed a two-site binding curve, which gave another higher affinity in the subpicomolar range.

Table 2

Null activity levels (mAmp displacement) in mice treated with vehicle, salvinorin A, or RB-64.

Treatment	Null Activity (mAmp displacement)
10% Tween Vehicle	11.16 ± 4.34
salvinorin A	
0.25 mg/kg	19.44 ± 5.83
0.5 mg/kg	28.79 ± 3.99*
1.0 mg/kg	13.63 ± 3.65
2.0 mg/kg	13.76 ± 3.65
RB-64	
0.005 mg/kg	8.22 ± 3.73
0.01 mg/kg	16.81 ± 4.4
0.05 mg/kg	64.89 ± 10.88*
0.1 mg/kg	51.6 ± 12.16*

* $p < 0.05$ compared to vehicle controls.